

STATUS REPORT ON THE RADIO FREQUENCY ACCELERATING SYSTEM OF THE APS AT ARGONNE\*

G. Nicholls, J. Bridges, J. Cook, and R. Kustom  
Argonne National Laboratory  
9700 S. Cass Avenue  
Argonne, IL 60439 USA

Argonne National Laboratory is designing a 7-GeV Advanced Photon Source (APS). The RF systems of the APS include 10-MHz and 120-MHz systems for the Positron Accumulator Ring (PAR), a multicell 352-MHz system for the booster synchrotron, and a system of mode-damped, single-cell 352-MHz cavities for the storage ring. This paper will describe the design of the PAR cavities, the configuration of the booster system, test results of the junction circulator developed for the cavities, and results of the higher-order mode damping as applied to the storage ring cavities.

Introduction

The positron beam is injected from an S-band linac into the PAR, bunched at the 36th and 3rd sub-harmonics of the synchrotron and storage ring RF frequency (351.9 MHz). Then it is injected into the synchrotron, accelerated to 7 GeV, and transferred to the storage ring. Table I lists the parameters of the various RF systems.

Table I  
DESIGN REQUIREMENTS FOR THE APS RF SYSTEMS

	Frequency MHz	Peak Voltage/Turn	Shunt Impedance Per Cavity	Number of Cavities	Total Required Power
PAR	9.8	40 kV	170 kΩ	1	4.7 kW
	117.3	30 kV	2020 kΩ	1	0.22 kW
Synchrotron	351.9	10.4 MV	65 MΩ	4 5-Cell (LEP TYPE)	625 kW
Storage Ring	351.9	6.5 MV	11 MΩ	15 Single Cell	2700 kW

Positron Accumulator Ring RF System

There are two RF systems in the PAR. One operates at 9.8 MHz and the other at 117 MHz. The control system also synchronizes operation with the linac during injection and with the injector synchrotron during extraction. The system is similar to that of PIA.<sup>1</sup>

The linac beam is injected into the 9.8-MHz bucket. The synchronous phase angle is about 175° to compensate for radiation loss while the bunch is damped. When the bunch is damped sufficiently, the 117-MHz system is turned on and further damping occurs until extraction.

The 117-MHz system is deactivated during the first 450-ms of the 500-ms PAR cycle to prevent self-bunching of the beam at 117 MHz.

The 9.8-MHz System

The 9.8-MHz cavity is a folded quarter-wavelength, coaxial re-entrant type that is capacitively loaded to resonate at a frequency of 9.8 MHz.

The cavity is made of aluminum with a ceramic cylinder across the accelerating gap for

\*This research was supported by the U.S. Department of Energy, Office of Basic Energy Sciences, under Contract W-31-109-ENG-38.

vacuum isolation. Only the beam tube is evacuated, keeping the vacuum system cost low and avoiding multipactoring problems in the bulk of the cavity. Fine tuning will be done by a capacitive adjustment located at the loading capacitor.

The power amplifier is located outside the shield wall but close enough to the cavity to minimize resonances in the transmission line.

Since beam loading is incremental, with 24 linac bunches injected over a 400-ms period, a modest feedback control system keeps the cavity voltage constant and the power amplifier load impedance real. Programming of the power amplifier input voltage and cavity fine tuning is included to offset the transient from each injected bunch. Feed-forward techniques can be added if necessary.

No higher-order-mode (HOM) suppression is included, although ports are available and could be used for mode-damping circuits.

The 117-MHz System

The 117-MHz cavity is a half-wavelength coaxial cavity slightly foreshortened by the accelerating gap capacitance. The cavity is made of aluminum, with the vacuum seal at the accelerating gap to minimize the vacuum volume and multipactoring difficulties. The cavity is tunable over a range of 1 MHz.

The cavity is electronically adjusted during operation of the 9.8-MHz cavity so as not to interact with the beam, since only the fundamental cavity is used during the injection time of the PAR cycle. PIN diodes are used to connect resistors coupled to the cavity to lower the gap impedance by at least a factor of ten. If needed, the resonance is shifted away from 117 MHz by similar PIN diode switches connecting a reactance into the cavity. Also, higher-order-mode suppression is implemented so that the beam is undisturbed during operation of the cavity.

When the cavity is switched from passive (imitating a beam pipe) to active state, beam loading is rapid. A fast tuning and voltage control system, including feed-forward techniques, is used. Large induced voltages (224 kV) are avoided with programmed tuning. The control circuit for the cavity uses both feedback signals from the cavity and feed-forward signals from a beam monitor. The amount of circulating beam controls the program signals to the power amplifier and to the tuning device, so that as the cavity is turned on for the last 50 ms of the PAR cycle, the accelerating voltage has the correct phase with respect to the 9.8-MHz bucket and the power amplifier sees a real load. The program can be a learning (adaptive) program to monitor the feedback error signals and adjust the program to minimize the errors. This correction can be done in several ways: over many PAR cycles, using only the last PAR cycle, or using a weighted running average. Using a correction signal improves the operation of the cavity and, for a given tolerance on cavity parameters, the feedback loop dynamic range and gain can be smaller.

The unloaded shunt impedance of the cavity is 2.0 MΩ and the maximum beam current is 112 mA, so the maximum induced voltage without compensation due to the beam is 224 kV. The RF amplifier produces a 30-kV accelerating voltage, and the total current without compensation would cause the voltage to be 82.4° out of phase with the empty 117-MHz buckets and the 9.8-MHz bucket. Since only 222 W is needed to power the empty cavity, resistive loading is added to the cavity to lower the shunt impedance and reduce the phase shift between beam current and generator current. This makes the programming and feedback systems less sensitive to variations in beam loading and increases the stability of the feedback system.

### Control and Synchronization

Since the rotation frequency, 9.7758 MHz, of the PAR is not an exact multiple of 60 Hz, the linac is triggered by the PAR control system at a nominal 60-Hz rate. This ensures that the subsequent linac beam pulses are in the same place in the bucket as the first beam pulse.

Similarly, the PAR is synchronized to the injector synchrotron RF at extraction so the bunch is correctly placed with respect to previous bunches in the 352-MHz buckets.

The 352-MHz frequency source has a resolution of 0.1 Hz without switching transients to prevent disturbing the stored beam. Two synthesizers are referenced to the 352-MHz source, one for each of the PAR cavities.

### Storage Ring System

Stability of the positron beam is strongly affected by the mode structure of the storage ring cavities. A prototype of the storage ring cavity is being fabricated (Varian Associates). It is designed for full power and high vacuum and will be used in studies of HOM suppression techniques.

### Computations Using MAFIA and URMEL

Geometry of the storage ring cavity has been modeled using URMEL<sup>2</sup> and MAFIA.<sup>3</sup> Results<sup>4</sup> are in agreement within the capability of the tuner. MAFIA runs indicate the tuning range of the tuning plunger is ± 0.5 MHz. Additional computations<sup>5</sup> indicate that the shunt impedance of some higher-order modes should be lowered (see Table II). We plan to shift modes that are coincident with exciting frequencies and to damp potentially troublesome modes.

### Field Measurement Techniques

As an aid to understanding the fields in the cavity, we have constructed a bead-pull system to measure longitudinal and transverse shunt impedance at the operating and HOM frequencies.

Several different formulae have been proposed for deducing field components from perturbations of resonant frequencies by metallic and dielectric beads. (See, for example, page 81 in Ref. 5, equations (52) through (70) in Ref. 6, §7-3 in Ref. 7, and §10.6 in Ref. 8.) All of these perturbation formulae are of the form

$$U \frac{\Delta\omega}{\omega} \approx \sum_{i=1}^3 (a_i |H_i|^2 - b_i |E_i|^2) \quad (1)$$

Table II. BUNCH STABILITY LIMITS

Mode	$f_r$	$R_s$ (MΩ)	$Q(x10^{-4})$	One Cavity Worst Case		15 Cavities Best Case	
				growth time $\tau_g$ (msec)	current limit $I_T$ (mA)	growth time $\tau_g$ (msec)	current limit $I_T$ (mA)
ME-1	540	3.35	4.2	5.32	23	157	751
EE-2	751	0.008	4.4	1807.5	6899	27155	116545
FE-3	923	1.20	10.6	21.1	91	644	2764
ME-2	948	0.464	4.4	22.1	95	240	1030
EE-4	1187	0.398	4.6	20.7	89	157	674
ME-3	1210	0.80	9.2	9.19	39	270	1159
EE-5	1326	0.018	12.5	412	1768	18360	78798
ME-4	1410	0.124	4.8	56.4	242	372	1597
EE-6	1505	1.0	8.6	8.58	28.2	107	459
ME-5	1545	0.013	9.2	494	2120	15350	65890

Calculations done for  $K_B = 20$  bunches. The worst case is for a single cavity with  $R_s$  and  $Q$  having a frequency  $f_r = (20p + s + V_s)/f_0$ .

The half integer case has 15 cavities with  $R_s$  (total) =  $15 \times R_s$ , and  $Q$  having a frequency  $f_r = (20p + s + 1/2)/f_0$  (i.e. midway between the closest revolution harmonic. (Kramer and Nicholls. Longitudinal EM Mode Calculation... APS/IN/RF/89-2)

where:  $\omega$  is the resonant frequency of the unperturbed mode,  $\Delta\omega$  is the shift of the frequency to that of the perturbed mode,  $U$  is the energy in the unperturbed mode,  $a_i$  and  $b_i$  are "form factors," and  $H_i$  and  $E_i$  are the complex magnetic and electric intensity vectors whose real parts are, after multiplication by  $\sqrt{2}e^{i\omega t}$ , components of the instantaneous fields with respect to a certain coordinate system fixed in the bead. It follows from very general assumptions that for arbitrary bead-shapes and permittivity and permeability distributions in the bead, a coordinate system in the bead can be found such that there will exist  $a_i$  and  $b_i$  for a perturbation expression of the above form. Their exact values for certain shapes have also been derived theoretically, but we have used these theoretical values only for general guidance. They are sensitive functions of shapes that we have not reproduced with high accuracy, and we have used other shapes for which exact analytic expressions are not available, so we have adopted the following phenomenological approach to their determination.

To calibrate the beads we use cavities in which the modes are known analytically. In particular, we have used the  $TM_{010}$  mode in a pill-box cavity. We estimate the  $a_i$  and  $b_i$  for each bead as the least-squares solution of the over-determined set of linear equations

$$U \frac{\Delta\omega}{\omega} = \sum_{i=1}^3 (a_{i,n} |H_{i,n}^{\text{Pill-Box}}|^2 - b_{i,n} |E_{i,n}^{\text{Pill-Box}}|^2) \quad (2)$$

where the subscript  $n = 1, \dots, N > 6$  denotes different positions and orientations of the bead. Included are three orientations at both the center of the cavity, where  $\vec{H} \approx \vec{0}$ , and at an off-axis position, where  $|\vec{H}| > |\vec{E}|$ . Other measurements at other positions and orientations and even other times, modes, and cavities (in which case  $U$  will depend on  $n$ ) are included in the same set of equations so that the least-squares program can give us a useful estimate of our experimental errors.

The mode will be a scalar multiple of one the energy of which has been analytically normalized to unity. The multiple can be determined by data from the same pickup on the cavity wall that is used to determine  $\Delta\omega$ .

After each bead has been calibrated by finding its  $a_i$  and  $b_i$ , we estimate the normalized ( $U = 1$ ) field quantities  $|H_i|^2$  and  $|E_i|^2$  at a given point in the cavity under investigation, as the least-squares solution of the over-determined set of linear equations

$$\frac{\Delta\omega_m}{\omega} = \sum_{i=1}^3 (a_{i,m}|H_i|^2 - b_{i,m}|E_i|^2) \quad (3)$$

where the subscript  $m = 1, \dots, M > 6$  ranges over beads and orientations. We solve the equations subject to the linear inequality constraints  $|H_i|^2 > 0$  and  $|E_i|^2 > 0$  by means of the program described in Ref. 9.

To pick the proper branch of the square-root function so that  $H_i = (|H_i|^2)^{1/2}$  and

$E_i = (|E_i|^2)^{1/2}$ , we use the fact that  $\vec{H}$  and  $\vec{E}$  are

solutions of the Helmholtz equation and hence have smooth derivatives of all orders in the interior of the cavity. Therefore, the second derivatives of  $|H_i|$  and  $|E_i|$  are Dirac  $\delta$ -functions at the sign-changes. Such singularities are well-defined even in a noisy numerical approximation, so it has been possible to automate the finding of the sign-changes in the field-plotting program.

We have made phase-shift measurements similar to those of Jacob<sup>10</sup> using an HP8510A network analyzer controlled by an HP Vectra computer.

#### Circulator

We plan to have a high power circulator at the input to each synchrotron and storage ring cavity. This circulator configuration will act in conjunction with our HOM suppressors to lower the unwanted HOM impedance and to prevent cross-coupling of RF energy from cavity to cavity.

We are purchasing a prototype circulator and have done high-power tests at SLAC on a 1/2-height WR 2300 junction circulator (Ferrite Components, Inc.). It initially used thermally sensitive magnetic shunts to adjust the magnetic field on the ferrite as operating conditions changed. Manual adjustment of the ferrite biasing field was required at a forward power level of 180 kW and again at 250 kW to keep the VSWR within specification (Max. 1.15). See Figure 1. Dynamic compensation is required. The manufacturer is developing such a system.

#### RF Test Station

We are presently assembling a high-power RF test station which will have a 250-kW RF source for testing the 352-MHz cavities and the high-power components (input power couplers, waveguide transitions, higher-order-mode suppressors, phase shifters, and matching devices.) The amplifier tube for this test station is being procured, and the power supply will be procured soon. The test station will be computer controlled and monitored, and is intended as a prototype of the system for both the synchrotron and storage ring. The test station will be completed in January 1990, and high-power tests will begin shortly thereafter.

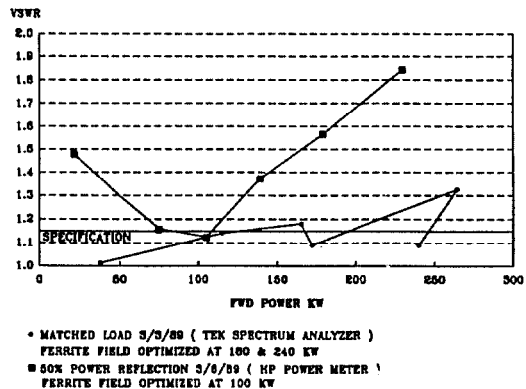


Fig. 1. Results of Circulator Test

#### References

1. Ebeling et al., Radio Frequency System of PIA, Particle Accelerator Conference 1981; IEEE NS-28 (1981).
2. T. Weiland, On the Computation of Resonant Modes in Cylindrically Symmetric Cavities, Nuclear Instruments and Methods, NIM, 216, pp. 329-348 (1983).
3. T. Weiland, On the Unique Numerical Solution of Maxwellian Eigenvalue Problems in Three Dimensions, Particle Accelerators, 17, pp. 227-242 (1985).
4. Y. Jin and G. Nicholls, Computations Predicting RF Cavity Characteristics, Argonne National Laboratory, APS Light Source, APS/LS-124.
5. J. C. Slater, Microwave Electronics, D. Van Nostrand Company, Inc., New York (1950).
6. L. C. Maier and J. C. Slater, Journal of Applied Physics, 23, p. 68 (1952).
7. R. F. Harrington, Time-Harmonic Electromagnetic Fields, McGraw-Hill Book Company, Inc., New York (1961).
8. E. L. Ginzton, Microwave Measurements, McGraw-Hill Book Company, Inc., New York (1957).
9. R. L. Crane, B. S. Garbow, K. E. Hillstrom and M. Minkoff, LCLSQ: An Implementation of an Algorithm for Linearly Constrained Linear Least-Squares Problems, Argonne National Laboratory Report, ANL-80-116 (1980).
10. J. Jacob, Measurement of the Higher Order Mode Impedance of the LEP Cavities, ESRF-RF/88-02, European Synchrotron Radiation Facility, Grenoble (1988).